Journal of the European Ceramic Society 20 (2000) 2063–2068

Grain boundary sliding-induced deformation in a 30 wt% zirconia–spinel composite: influence of stress

A. Addad [a], J. Crampon [a], R. Guinebretière [b], A. Dauger [b], R. Duclos [a,*]

[a] *Laboratoire de Structure et Propriétés de l'Etat Solide, ESA 8008, Bât. C6, Université des Sciences et Technologies de Lille, 59655 Villeneuve d'Ascq Cedex, France*

[b] *Laboratoire de Science des Procédés Céramiques et de Traitement de Surface, UMR 6638, ENSCI, 47 avenue Albert Thomas, 87065 Limoges Cedex, France*

Received 1 November 1999; received in revised form 15 February 2000; accepted 18 February 2000

Abstract

The contribution of grain boundary sliding to total strain has been investigated in a 21 vol% zirconia–spinel composite crept under stresses of 12 and 90 MPa. To this goal, the surface topography and its changes with strain were investigated on a face parallel to the compression axis by atomic force microscopy in contact mode. Due to the low zirconia content, only sliding on spinel–spinel (S–S) and spinel–zirconia (S–Z) boundaries really contributes to strain and was consequently analysed. Insensitive to stress value, boundary sliding can account for 70–80% of the total strain. However, if the two investigated interfaces behave similarly at 90 MPa, at 12 MPa sliding on S–Z boundaries is larger than on S–S ones. That difference is to relate to a stress–strain rate sensitivity dependent on stress, 1.8 and 4.2 at 90 and 12 MPa, respectively, an increase in the stress exponent able to be induced by the existence of a threshold stress that would concern spinel–spinel boundaries.

Keywords: Atomic force microscopy; Grain boundaries; Plasticity; Spinel; ZrO_2

1. Introduction

The role played by grain boundaries during the superplastic deformation of materials is of prime importance. Concerning metallic alloys for instance, it has been shown that grain boundary sliding is the rate controlling mechanism in the superplastic region II of the stress–strain rate diagram and may account for the essential of the total strain.[1] Comparatively, grain boundary sliding seems to be less active in the low stress region I. This may result from grain boundary impurity segregation that affects the movement of grain boundary dislocations.[2] Thus, in the case of the superplastic Pb–62%Sn eutectic, Vastava and Langdon[3] reported that the contribution of grain boundary sliding to total strain is about 50–60% in the region II while it decreases to only 20% in the region I, values in concordance with those measured in other superplastic metallic alloys (see [4] for instance).

Though results relating to ceramics are less documented, it is likely that the above conclusions are roughly valid for this kind of material, grain boundary sliding being able to contribute to more than 70% of the total strain of fine-grained ceramics for certain deformation conditions.[5–7]

This work is devoted to the investigation of grain boundary sliding in a zirconia–spinel composite tested under two stress levels for which very different stress sensitivities of the creep rate $\dot{\varepsilon}$ (n in the equation: $\dot{\varepsilon} = A\sigma^n$, with σ the stress) were established: n is about 1.5–2 for stresses higher than 70 MPa while it increases to values as high as 5 when the stress is reduced to 10 MPa.[8,9] This observation is often ascribed to a threshold stress[2,10,11] that must be exceeded to allow material deformation. In the present case, understanding of this behaviour needs first to know whether one kind of boundary is more specially implied in its origin, three types of interfaces being able to contribute to boundary sliding in a two-phase material. Determination of the sliding capability of various interfaces, a fundamental property of grain boundaries with respect to plastic deformation, is able to give useful information about

* Corresponding author. Tel.: +33-3-2043-4990; fax: +33-3-2043-6591.

E-mail address: Richard.Duclos@univ-lille1.fr (R. Duclos).

0955-2219/00/$ - see front matter
PII: S0955-2219(00)00079-0

this origin and will allow to select, for instance, the kind of boundary that should be investigated by high resolution transmission electron microscopy or analytical microscopy. In the material selected for this study, owing to the reduced volume ratio of zirconia phase (21%), zirconia–zirconia boundaries are much fewer than spinel–spinel (S–S) and spinel–zirconia (S–Z) interfaces (~3% of all boundaries) and do not really contribute to deformation. Consequently, grain boundary sliding determination has been focused on S–S and S–Z interfaces. To this end, owing to the fine grain sizes of composite (~1 μm) that do not allow the use of conventional methods as interferometry or measurement of offset of marker lines, an atomic force microscope (AFM) has been used to investigate the changes in surface topography with deformation, a technique that has already proved its ability in the case of two fine-grained ceramic materials, a single phase alumina[6] and a zirconia–alumina composite.[7]

2. Experimental procedure

The 30 wt% ZrO_2–$MgAl_2O_4$ composite was prepared by a technique already described[12] that consists in coating crystalline spinel particles of a commercial powder (Baikowski S30CR, Annecy, France) with a zirconia precursor. After drying and firing of the coated powder, disks were cold pressed and then sintered at 1550°C during 1 h. This resulted in a nearly fully densified material (about 99% of the theoretical density) in which the distribution of zirconia particles in the spinel matrix is very homogeneous. Fig. 1 is a scanning electron micrograph (SEM) which shows the distribution of the two phases. Zirconia particles are mainly located at triple points of the spinel phase. The mean intercept values of spinel and zirconia grains are $\overline{L}_S = 0.46$ μm and $\overline{L}_Z = 0.40$ μm, respectively.

Compressive creep tests were performed in air at 1380°C under stresses of 12 and 90 MPa up to strains of 18 and 15% respectively. These strains are large enough to produce a meaningful sliding contribution but not too important to avoid difficulties in the analysis of surface relief changes. Specimen size was 3×3×7 mm. Prior to creep, one of the side face was diamond polished and annealed. Then several 10×10 μm areas were examined by AFM in contact mode with a pyramidal Si_3N_4 tip, at constant deflexion of the cantilever. In these working conditions, the AFM is used as a high resolution profilometer.[6] Presently, we have checked that this mode did not introduce artefacts able to strongly modify the surface profile relative to the real one[13] (in particular no abrasion of the specimen surface was observed) except those inherent in the tip shape whose influence on the surface topography can be foreseen.[14] After completion of the test, the same zones as those examined prior to creep were again analysed. Then, the sliding component perpendicular to the specimen surface (the v component in Fig. 2) was determined by comparing the surface profile perpendicularly to the same boundaries on images recorded before and after deformation.

Two examples are presented in Fig. 3a and b. In the first case when the interface is surrounded by two large grains, the average surface of each grain is adjusted by a plane. The magnitude of the sliding component v, carried out according to Fig. 3a, corresponds to the change in step height (in absolute value) that occurred during deformation (here $|v_0 + v_{15}|$). In the second case when small grains were implied, (frequently zirconia grains) their surface was often curved. The top of the grain was taken as reference as Fig. 3b shows; the component v is then equal to $|v_{18} - v_0|$. In addition, these examples are revealing of the grain rotation happening during deformation.

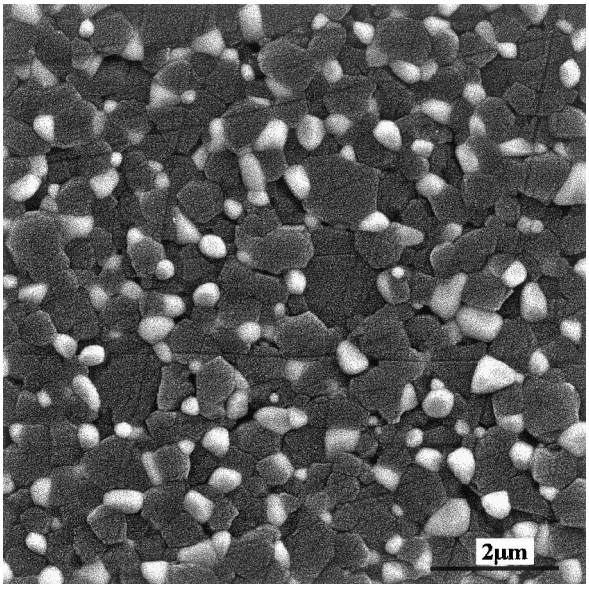

Fig. 1. Backscattered electron micrograph showing the distribution of the two phases. Dark grains are the spinel ones.

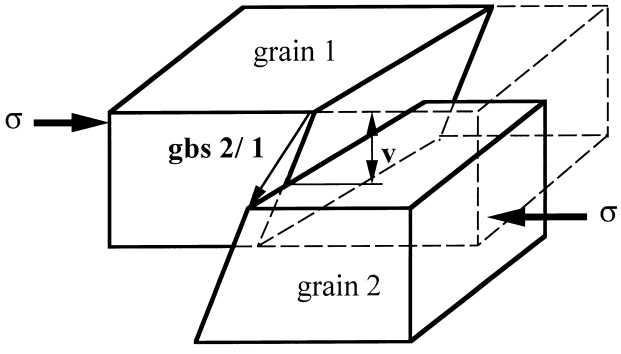

Fig. 2. Representation of the component v of the grain boundary sliding.

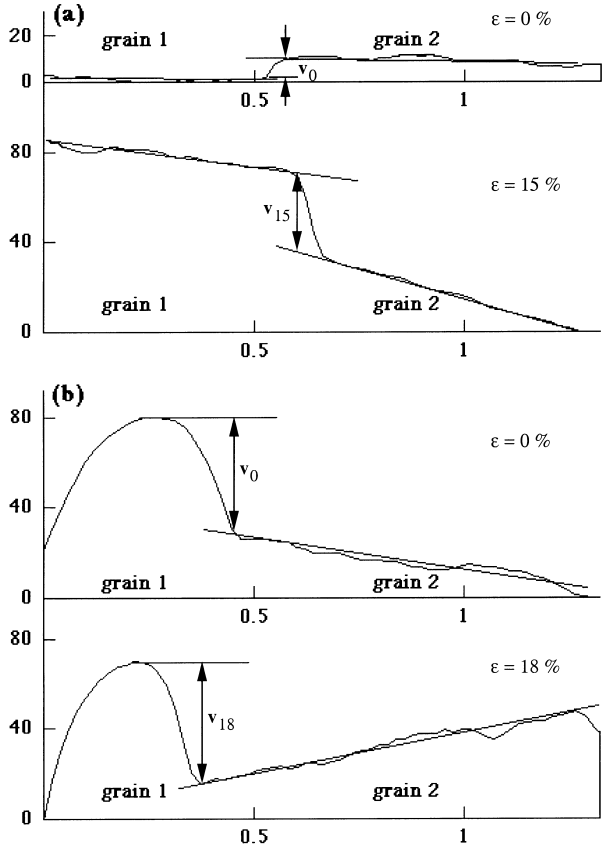

Fig. 3. Two examples presenting the method used to determinate the grain boundary sliding component v: (a) case of two spinel grains and (b) case of a spinel grain (2) and a zirconia grain (1). Horizontal scales in μm, vertical scales in nm.

In each 10×10 μm analysed area (5 areas were examined in each specimen corresponding to more than 250 boundaries of each kind), the selected boundaries were those intercepted by nine equidistant lines (~1.1 μm) parallel to the compression axis; this procedure allows the preservation of the haphazard characteristic of the method.[6,15]

3. Experimental results

Fig. 4 shows the stress–strain rate diagram for this material and the experimental stress conditions corresponding to n values of 1.8 ($\sigma = 90$ MPa) and 4.2 ($\sigma = 12$ MPa). These stress values have been chosen to avoid both grain coarsening and cavity formation that would disturb grain distribution. The changes in topography associated with deformation at 12 and 90 MPa are presented in Figs. 5 and 6, respectively. In these figures, the grey level accounts for the z coordinate, the one perpendicular to the image plane. By comparing images prior to and after creep the effect of deformation is clearly visible: surface roughness and the z range

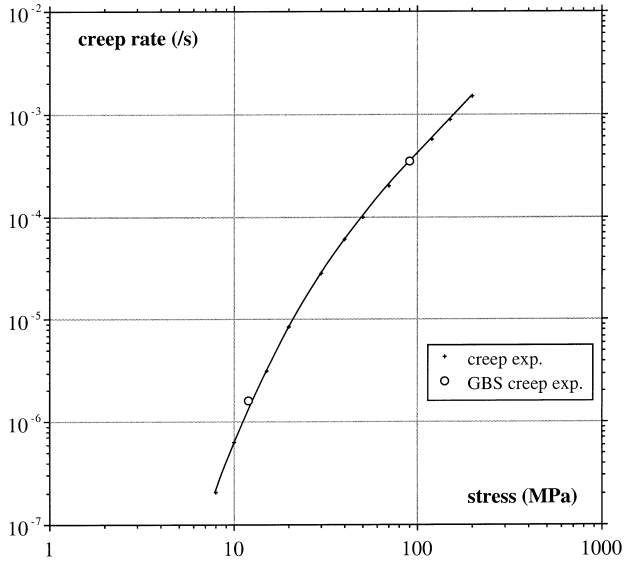

Fig. 4. The stress–strain rate curve showing the continuous decrease in stress exponent when stress increases; the two experimental stresses have been indicated.

increased which renders perceptible grain boundary sliding. Owing to the absence of information about the grain phase (spinel or zirconia) in AFM images, this technique was systematically coupled with SEM (Fig. 5c). From comparison of Fig. 5b and c, it can be seen that, because of the tip shape, prominent grains appear slightly larger on the AFM image than on the SEM one. Determination of the vertical grain boundary sliding component is almost insensitive to this artefact.

From measurements of the component v, the distribution functions have been calculated for the two types of interfaces. Increments of 20 nm has been considered. The results are presented in Fig. 7a and b that compare the sliding behaviour of each interface at 12 and 90 MPa, respectively. Table 1 recapitulates for the S–S and S–Z boundaries, and for the composite too, the mean value ⟨v⟩ of the vertical component v, the corresponding sliding rate $\mathrm{d}\langle v\rangle/\mathrm{d}t$, the strain $\varepsilon_{\mathrm{gbs}}$ induced by grain boundary sliding and the resultant contribution to the total deformation $\gamma = \varepsilon_{\mathrm{gbs}}/\varepsilon_{\mathrm{tot}}$. The strain $\varepsilon_{\mathrm{gbs}}$ was estimated from the relation proposed by Langdon:[15,16]

$$\varepsilon_{\mathrm{gbs},\,i} = 1.4\langle v_i\rangle/\overline{\mathrm{L}}_i \qquad (1)$$

in which the subscript i refers to the type of interface (S–S or S–Z). The calculated value from relation (1) corresponds to a material where only this kind of interface would be present. For the S–Z interphase boundaries the mean intercept value was taken as 0,5 ($\overline{L}_{\mathrm{S}} + \overline{L}_{\mathrm{Z}}$). Moreover, in the case of the composite, the average value $\langle v\rangle$ was calculated by taking into consideration the interception frequency of each type of interface (S–S: 52%; S–Z: 48% and Z–Z: neglected).

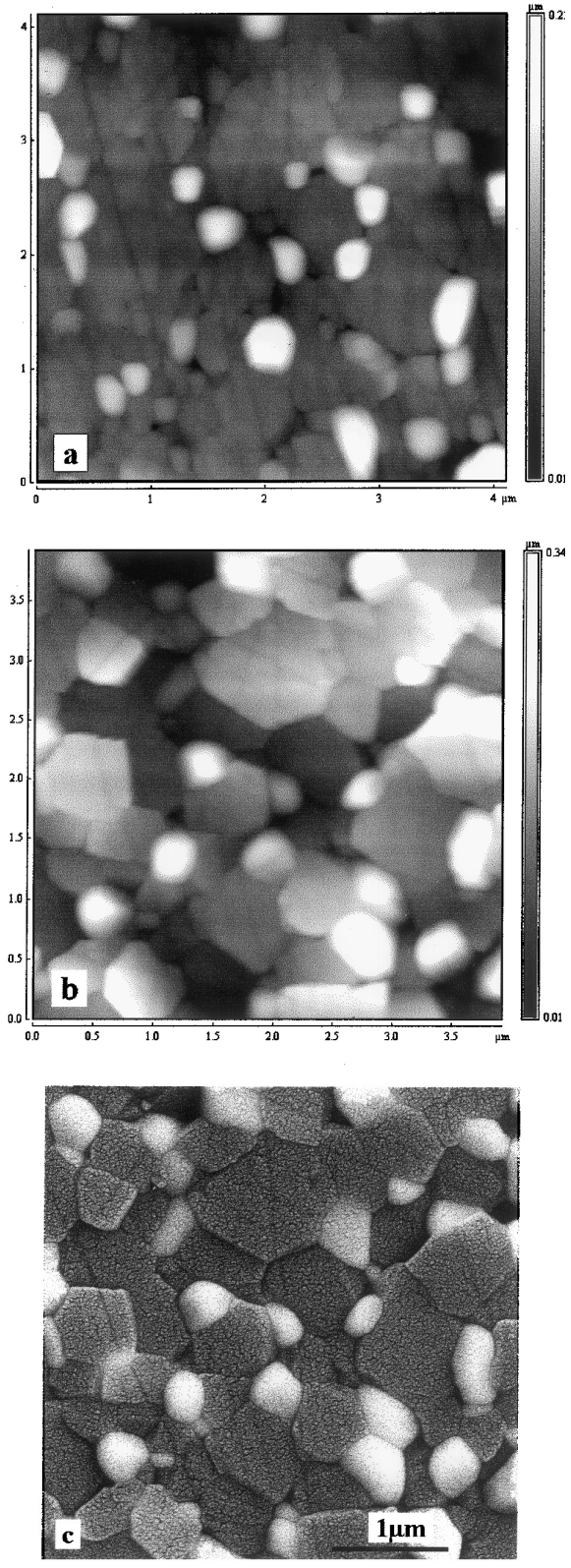

Fig. 5. AFM images of a 4×4 μm area: (a) prior to creep, (b) after a creep strain of 18% under 12 MPa and (c) the corresponding SEM image in the strained state. Note the slight topography difference between (b) and (c).

4. Discussion

Reliability and limitation of this method have been already discussed.[6,7] Concerning the number of boundaries investigated in this work (more than 250 of each type), it is high enough to be representative of the whole composite. With respect to performed strains, examination of the same boundaries requires that changes in surface topology are absent or weak, which necessary limits the ultimate strains to about 20%. However experiments performed in the Zn–22%Al eutectic[4] showed that results obtained in a low strain range (up to 50%) or at higher elongations (200%) are very similar. One can then believe that present results would be still valid for larger strains. We would like to add, in the present case, that difficulty arose from a bad boundary grooving by thermal etching. This issues from the low surface diffusivity in the spinel phase for annealing conditions that preserve the material grain sizes.

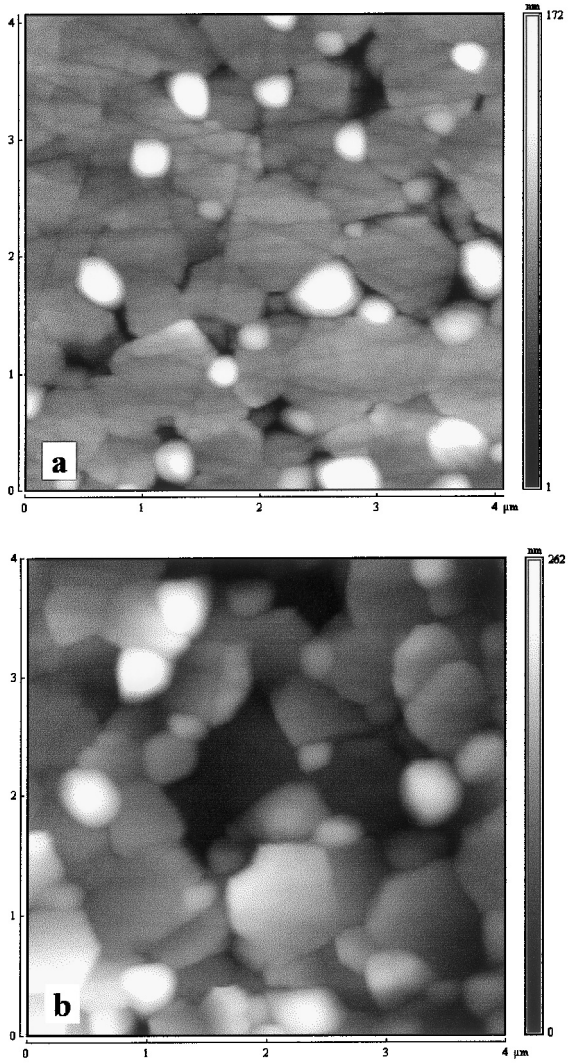

Fig. 6. AFM images of a 4×4 μm area: (a) prior to creep and (b) after a creep strain of 15% under 90 MPa.

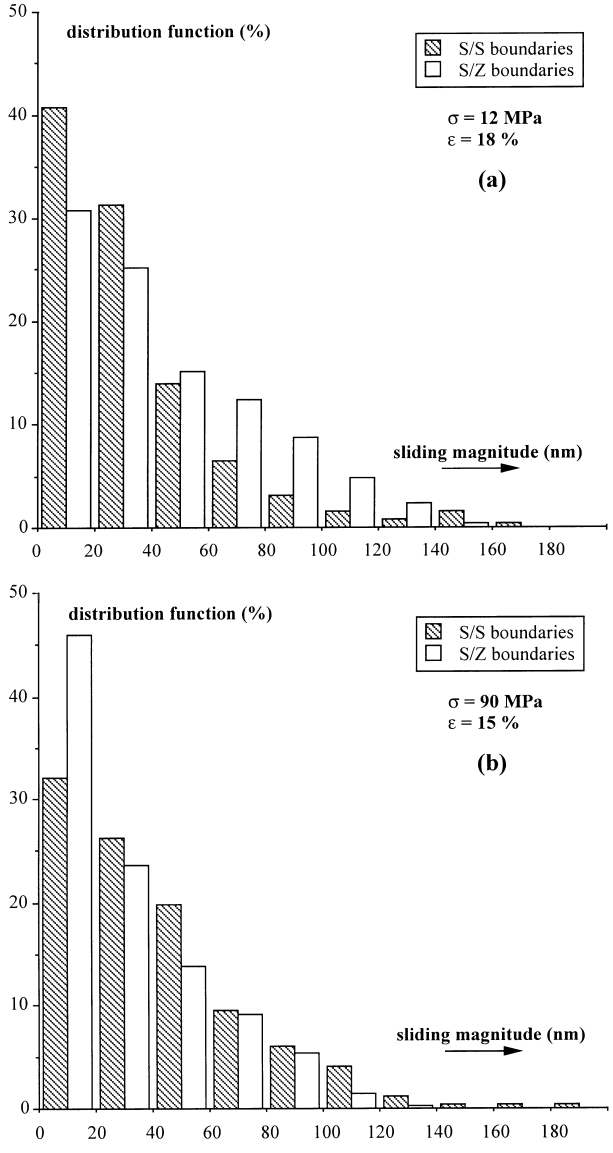

Fig. 7. Distribution functions comparing the sliding behaviour of the two types of interface at (a) 12 MPa and (b) 90 MPa.

Two kinds of information arise from Fig. 7 and Table 1. The first one concerns the average behaviour of boundaries in the composite. At 12 and 90 MPa grain boundary sliding contributes to about 70 and 80% of the total strain respectively. On the one hand these values show the importance of grain boundary sliding in the composite deformation, even at low stress when the stress exponent exhibits an unusual high value. On the other hand, owing to measurement scattering, the two values are very similar, contrary to observations in metallic alloys.[4] This demonstrates that at 12 MPa (at 1380°C the threshold stress has been estimated to about 5–6 MPa[8,9]) an intragranular deformation mechanism, such as dislocation glide or a pure diffusion creep, did not take the place of grain boundary sliding when this one appears to be more difficult than at 90 MPa.

The second information is relative to the particular sliding capability of each type of interface. The two investigated boundaries behave differently as a function of the stress level. At 90 MPa the two distribution functions are about similar and lead to equivalent contributions of S–S and S–Z boundaries to total strain. On the contrary, the distribution functions at low stress strongly differ: the sliding contribution on S–Z interphase boundaries is larger than on S–S interfaces. In the low stress range spinel–zirconia boundaries are more suited to slide than spinel–spinel ones and balance the weaker contribution of spinel–spinel boundaries to total strain, an increasing contribution of an intragranular deformation mechanism not being observed. Moreover, the difference in sliding capability is likely more marked than that reported in Table 1. Effectively, the measured sliding magnitude for a given interface is depending upon its surroundings and the stress redistribution acting during the creep test. As an increase in zirconia content improved the composite ductility,[8,9] one can conclude that the spinel phase is the less plastic one. Consequently, it is likely that the applied stress is mainly transferred on the spinel phase during deformation, which favours

Table 1
Main characteristics of grain boundary sliding (gbs)

Interface[a]	Spinel–spinel		Spinel–zirconia		Composite	
Stress (MPa)[b]	12	90	12	90	12	90
Total strain (%)[b]	18	15	18	15	18	15
$\langle v \rangle$ (nm)[c]	33±4	40±3	44±7	32±5	38±5	36±4
Sliding rate (nm.s^{-1})[d]	3.3*10^{-4}	8.3*10^{-2}	4.4*10^{-4}	6.7*10^{-2}	3.8*10^{-4}	7.5*10^{-2}
ε_{gbs} (%)[e]	10	12	15.3	11	12.6	12
γ (%)[f]	55±7	80±6	85±13	74±11	70±9	80±9

[a] The first line refers to the type of interface; in the case of "composite" it is a mean interface that is considered (52% S–S + 48% S–Z).
[b] The second and third lines recall the deformation conditions, stress and total strain.
[c] The fourth line reports the average value of component v.
[d] The sliding rate in line five is obtained by dividing $\langle v \rangle$ by the test duration (10^5 s and 480 s at 12 and 90 MPa, respectively).
[e] In the sixth line the deformation resulting from gbs is calculated according to relation (1).
[f] Finally the seven line presents the contribution γ of gbs to total strain. In addition the measurement incertitude is the standard deviation of the five average values obtained from measurements performed in each analysed area.

sliding on spinel–spinel boundaries relative to spinel–zirconia ones. Stress redistribution could be analysed from these experiments if the sliding behaviour of spinel phase boundaries was known.[7]

The experimental results confirm that deformation mainly results from grain boundary sliding but that boundaries responsible for sliding are dependent on the stress level. Due to the large spinel volume fraction and the absence of an additional intragranular deformation mechanism, the decrease in sliding capability of the spinel–spinel boundaries results in a corresponding decrease in the creep rate that induces the observed increase in stress exponent at low stress. On the other hand, the decrease in sliding capability of S–S interfaces at low stress is probably able to entail a threshold stress, the very fine grain sizes of the composite being a favourable condition for such an occurrence. Nevertheless, the present experiments do not allow to establish unambiguously the origin of such a threshold. They just constitute an information that must be taken into consideration in the analysis of the composite creep behaviour as boundary investigations, by TEM for instance to account for geometry and chemistry, or macroscopic thermomechanical parameters are. This is in due course.

Present contributions of grain boundary sliding are similar to those determined in single or two-phase ceramic materials with grain sizes in the range 1 to a few μm,[5–7] i.e. about 70–80%. These values confirm that deformation of fine-grained ceramic materials is only weakly dependent on intragranular mechanisms. This originates from the absence of bulk dislocations and the high stresses required to move them when they are present,[17] a feature very different from that of metallic alloys.

5. Conclusion

Atomic force microscopy, used as a high resolution profilometer, allowed us to investigate the sliding capability of spinel–spinel and spinel–zirconia interfaces in a 30 wt% zirconia–spinel ceramic, crept under two stresses of 12 and 90 MPa, by measuring the magnitude of the sliding component perpendicular to the specimen surface. The contribution of sliding to total strain is high (~70–80%) whatever stress, in agreement with earlier data on fine-grained ceramics. Nevertheless, the two investigated interfaces behave differently, depending on stress level. At high stress (90 MPa) S–S and S–Z boundaries exhibit similar sliding possibilities while at low stress (12 MPa) sliding on spinel–zirconia interfaces is larger than on spinel–spinel ones. This decrease in sliding capability of S–S interfaces at low stress is to relate to the increase in stress exponent in this stress range that may originate from a threshold stress, the composite grain sizes being propitious to the occurrence of such a threshold. However, the origin of this threshold, in the region of a few MPa, cannot be directly deduced from these experiments and requires subsequent work.

References

1. Langdon, T. G., The role of grain boundaries in high temperature deformation. *Mat. Sci. Eng.*, 1993, **A166**, 67–79.
2. Mohamed, F. A., Interpretation of superplastic flow in terms of a threshold stress. *J. Mater. Sci.*, 1983, **18**, 582–592.
3. Vastava, R. B. and Langdon, T. G., An investigation of intercrystalline and interphase boundary sliding in the Pb-62% Sn eutectic. *Acta Metal.*, 1979, **27**, 251–257.
4. Lin, Z.-R., Chokshi, A. H. and Langdon, T. G., An investigation of grain boundary sliding in superplasticity at high elongations. *J. Mater. Sci.*, 1988, **23**, 2712–2722.
5. Chokshi, A. H., An evaluation of the grain boundary sliding contribution to creep deformation in polycrystalline alumina. *J. Mater. Sci.*, 1990, **25**, 3221–3228.
6. Clarisse, L., Bataille, A., Pennec, Y., Crampon, J. and Duclos, R., Investigation of grain boundary sliding during superplastic deformation of a fine-grained alumina by atomic force microscopy. *Ceram. Inter.*, 1999, **25**, 389–394.
7. Clarisse, L., Petit, F., Crampon, J. and Duclos, R., Characterization of grain boundary sliding in a fine-grained alumina-zirconia ceramic composite by atomic force microscopy. *Ceram. Inter.*, 2000, **26**, 295–302.
8. Addad, A., Study of the high temperature plasticity of spinel-zirconia ceramics (in French), PhD thesis, Université des Sciences et Technologies de Lille, France, 1999.
9. Addad, A., Crampon, J. and Duclos, R., High temperature deformation of spinel–zirconia composites: grain boundary sliding accommodation, submitted to *Mater. Sci. Eng.*
10. Duclos, R. and Crampon, J., Diffusional creep of a SiC whisker reinforced alumina/zirconia composite. *Scripta Metal.*, 1989, **23**, 1673–1678.
11. Bravo-Léon, A., Jiménez-Melendo, M. and Dominguez-Rodriguez, A., The role of a threshold stress in the superplastic deformation of fine-grained yttria-stabilized zirconia polycrystals. *Scripta Mater.*, 1996, **34**, 1155–1160.
12. Guinebretiére, R., Masson, O., Ruin, P., Trolliard, G. and Dauger, A., Sol gel coating of ceramic powders. *Phil. Mag. Let.*, 1994, **70**, 389–396.
13. Grütter, P., Zimmermann-Edling, W. and Brodbeck, D., Tip artefacts of microfabricated force sensors for atomic force microscopy. *Appl. Phys. Lett.*, 1992, **60**, 2741–2743.
14. Westra, K. L., Mitchell, A. W. and Thomson, D. J., Tip artefacts in atomic force microscope imaging of thin film surfaces. *J. Appl. Phys.*, 1993, **74**, 3608–3610.
15. Langdon, T. G., The effect of surface configuration on grain boundary sliding. *Metal. Trans.*, 1972, **3**, 797–801.
16. Langdon, T. G., Grain boundary deformation process. In *Deformation of Ceramic Materials*, ed. R. C. Bradt and R. E. Tressler. Plenum Press, New York, 1975, pp. 101–126.
17. Duclos, R., Doukhan, N. and Escaig, B., Study of the origin of the composition influence on the mechanical properties of $MgO.nAl_2O_3$ spinels. *Acta Metal.*, 1982, **30**, 1381–1388.